Electrical stiffness tuning in ferromagnetic shape memory Ni-Mn-Ga

Neelesh N. Sarawate[a], Marcelo J. Dapino[a]

[a] Department of Mechanical Engineering,
The Ohio State University, Columbus, OH, USA, 43210

ABSTRACT

This paper is focused on the dynamic characterization of field-induced mechanical stiffness changes under varied bias magnetic fields in commercial-quality, single-crystal ferromagnetic shape memory Ni-Mn-Ga. Prior to the dynamic measurements, a specified variant configuration is created in a prismatic Ni-Mn-Ga sample through the application and subsequent removal of collinear or transverse bias magnetic fields. Base excitation is used to measure the acceleration transmissibility across the sample, from where the resonance frequency is directly identified. These measurements are repeated for various collinear and transverse bias magnetic fields ranging from 0 to 575 kA/m, which are applied by a solenoid and an electromagnet, respectively. A 1-DOF model for the Ni-Mn-Ga sample is used to calculate the mechanical stiffness from resonance frequency measurements. A resonance frequency increase of 21% and a stiffness increase of 52% are observed in the collinear field tests. In the transverse field tests, a resonance frequency decrease of -36% is observed along with a stiffness decrease of -61%. The damping exhibited by this material is low in all cases (≈ 0.03). The measured dynamic behaviors make Ni-Mn-Ga well suited for vibration absorbers with electrically-tunable stiffness.

Keywords: Ferromagnetic shape memory, Ni-Mn-Ga, stiffness tuning, dynamic characterization, vibration control

1. INTRODUCTION

Ferromagnetic shape memory alloys exhibit large strains and relatively high bandwidth, which are attractive characteristics for actuator design. Most of the work on these materials has been focused on the quasistatic characterization and modeling of Ni-Mn-Ga for actuation applications. The investigation of applications other than actuation has been limited, and has been largely been focused on sensing. Mullner et al.[1] experimentally studied strain-induced changes in the flux density of a single crystal with composition $Ni_{51}Mn_{28}Ga_{21}$ under external quasistatic loading at a constant field of 558 kA/m. Straka and Heczko[2] reported superelastic response of a $Ni_{49.7}Mn_{29.1}Ga_{21.2}$ single crystal with 5M martensitic structure for fields higher than 239 kA/m and established the interconnection between magnetization and strain. Heczko[3] further investigated this interconnection and proposed a simple energy model. Li et al.[4] reported the effect of magnetic field during martensitic transformation on the magnetic and elastic behavior of $Ni_{50.3}Mn_{28.7}Ga_{21}$. Suorsa et al.[5] reported magnetization measurements conducted on stoichiometric Ni_2MnGa material for various discrete strain and field intensities ranging between 0–6 % and 5–120 kA/m, respectively. Sarawate and Dapino[6] showed that commercial Ni-Mn-Ga is viable for high-compliance, high-displacement deformation sensors. Their measurements show an almost linear range of flux density change of 0.25 T when the material is subjected to 5% strain and 2.2 MPa stress. These metrics were obtained at a bias field of 173 kA/m and a bias stress of 2.2 MPa.

This paper is focused on the dynamic stiffness tuning of commercially available Ni-Mn-Ga (Adaptamat Inc.), with a view to developing tunable vibration absorbers. In the low temperature martensite phase, the material exhibits a twin variant microstructure consisting of field and stress preferred variants. At large field magnitudes (> 700 kA/m) or large compressive stresses (> 3 MPa), the material respectively becomes a single field-preferred variant or single stress-preferred variant. The quasistatic stress-strain curve[6] shows that the stiffness of the two different configurations is significantly different. At intermediate fields and stresses, both variants are present in

Further author information: (Send correspondence to M.J.D)
N.N.S.: E-mail: sarawate.1@osu.edu, Telephone: 1-614-247-7480
M.J.D.: E-mail: dapino.1@osu.edu, Telephone: 1-614-688-3689

Sensors and Smart Structures Technologies for Civil, Mechanical, and Aerospace Systems 2007,
edited by Masayoshi Tomizuka, Chung-Bang Yun, Victor Giurgiutiu, Proc. of SPIE Vol. 6529,
652916, (2007) · 0277-786X/07/$18 · doi: 10.1117/12.715927

Downloaded From: http://proceedings.spiedigitallibrary.org/ on 07/12/2017 Terms of Use: http://spiedigitallibrary.org/ss/termsofuse.aspx

the twin variant structure and the material exhibits a bulk stiffness between the two extreme values. This offers the opportunity to control the bulk material stiffness through control of variant volume fractions by application of fields and stresses. It is noted that application of magnetic fields is the preferred method of controlling the stiffness, as it is a non contact method. From a control viewpoint, it is easy to control the magnetic field by varying the current supplied to a solenoid or an electromagnet.

Prior work by Faidley et al.[7] was conducted on research-grade Ni-Mn-Ga driven with magnetic fields applied along the [001] (collinear) direction. The fields were applied with permanent magnets stacked on the sample, which required the reliance on analytical models to distinguish resonance frequency changes due to magnetic fields from those due to mass increase.

In this paper, the magnetic fields are applied in the collinear and transverse direction using a solenoid coil and electromagnet, respectively, thus allowing the direct identification of resonance frequency shits. Base excitation is used to measure the acceleration transmissibility across a prismatic Ni-Mn-Ga sample, from where the resonance frequency is directly identified. The tests show the variation of the resonance frequency of the sample with changing *initial* bias field (the variant configuration is adjusted through the application and subsequent removal of a bias field prior to the transmissibility measurements). The change in twin variant configuration associated with changing bias fields results in a change in mechanical stiffness and hence, resonance frequency. The damping exhibited by the system in these dynamic tests is very low, which is advantageous for vibration absorber design.

The crystals with the c-axis in the longitudinal direction are termed stress-preferred variants, whereas the crystals with the c-axis in the transverse direction are called field-preferred variants (Figure 1). Due to the high magnetocrystalline anisotropy of Ni-Mn-Ga, the magnetization vectors tend to attach to the c-axis of the crystals, making this the easy magnetic axis. When a magnetic field is applied, the magnetization vectors try to rotate in the direction of the applied field in order to minimize the net Zeeman energy. As a result, the number of crystals with the c-axis oriented in the direction of the field grows at the expense of the number of crystals with the c-axis perpendicular to the applied field. When a longitudinal magnetic field is applied, the stress-preferred variants grow at the expense of field-preferred variants; the reverse is true when a transverse field is applied.

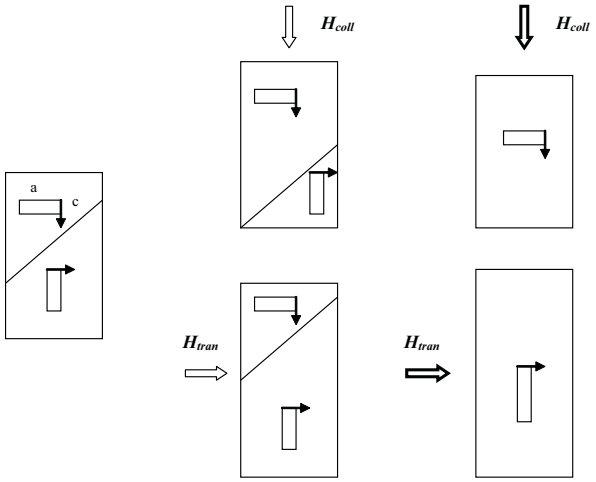

Figure 1. Schematic of the twin variant microstructure in Ni-Mn-Ga.

2. EXPERIMENTAL SETUP AND PROCEDURE

The measurements are conducted on single-crystal Ni-Mn-Ga produced by Adaptamat, Inc. A sample with dimensions 6 x 6 x 10 mm^3 is tested in its martensite phase. The sample exhibits 5.8% free strain in the presence of transverse fields of about 550 kA/m. For the mechanical excitation, a Labworks ET126-B shaker table is used

Downloaded From: http://proceedings.spiedigitallibrary.org/ on 07/12/2017 Terms of Use: http://spiedigitallibrary.org/ss/termsofuse.aspx

which has a frequency range of dc to 8500 Hz and a 25 lb peak sine force capability. The shaker is driven by an MB Dynamics SL500VCF power amplifier, with power of 1000 VA, and maximum voltage gain of 48 with 40 V peak and 16 A rms. The shaker is controlled by a Data Physics SignalCalc 550 vibration controller.

A schematic of the test setup for collinear tests is shown in Figure 2. The sample is mounted on an aluminum pushrod fixed on the shaker table, whereas a dead weight is mounted on top of the sample. Two PCB accelerometers measure the base and top accelerations. The collinear field is applied by a custom made water cooled solenoid transducer which is made from AWG 15 insulated copper wire with 28 layers and 48 turns per layer.[8] The solenoid is driven by two Techron 7790 amplifiers connected in series which produce an overall voltage gain of 60 and maximum output current of 56 A into the 3.7 Ω resistance of coil. The solenoid has a gain of 11.26 (kA/m)/A.

A schematic of the test setup for the transverse field tests in shown in Figure 3. A custom-made electromagnet is used to apply transverse fields, which is made from laminated E-cores with 2 coils of about 550 turns each made from AWG 16 magnet wire. The coils are connected in parallel. The electromagnet has a gain of 63.21 (kA/m)/A; it can produce fields of up to 750 kA/m.

For the collinear field tests, the sample is initially configured as a single field-preferred variant. The structure of the sample can be changed with increasing collinear fields by favoring the growth of stress-preferred variants, which results in a stiffening with increasing magnetic field. The sample in zero-field condition is first subjected to a random signal with a frequency range from 70 Hz to 4000 Hz and reference acceleration of 0.2 g (no significant

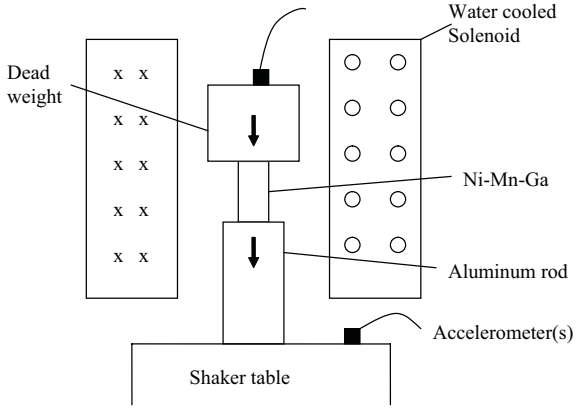

Figure 2. Schematic of the longitudinal field test.

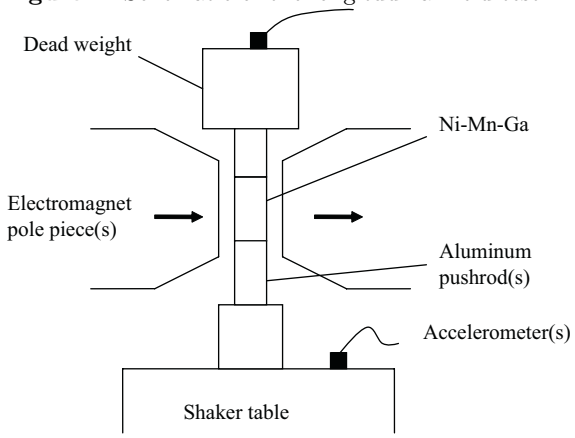

Figure 3. Schematic of the transverse field test.

Downloaded From: http://proceedings.spiedigitallibrary.org/ on 07/12/2017 Terms of Use: http://spiedigitallibrary.org/ss/termsofuse.aspx

dynamic activity is present below 70 Hz). After completion of the zero-field test, a DC voltage is applied across the solenoid to produce a DC collinear field on the sample. Due to the fast response of Ni-Mn-Ga,[9] application of the field for a small time period (about 1 to 2 seconds) is enough to change the variant configuration. If the field is strong enough to initiate twin boundary motion, stress-preferred variants are generated from the original field-preferred variants. The sample is again subjected to random excitation to record the top and base accelerations, from which the transfer function of the top acceleration to base acceleration can be obtained. This process is continued until the sample reaches a complete stress-preferred variant state. The maximum field applied to the sample is 430 kA/m. The tests are repeated several times.

For the transverse field tests, the sample is initially configured as a single stress-preferred variant. This configuration can be obtained by applying a high collinear field of 430 kA/m. The sample is mounted on the shaker table using aluminum pushrods between the pole faces of the electromagnet, and a dead weight is used. The test procedure is the same as in the collinear field test: the transverse bias field is incremented by a small amount and subsequently removed before each run. When the field is sufficiently high, field-preferred variants are generated at the expense of stress-preferred variants. It is noted that the maximum bias field applied of 575 kA/m is higher than in the collinear tests to compensate for the higher demagnetization factor.

3. THEORY

The system can be represented by the second-order system shown in Figure 4, where K_s represents the stiffness of the sample, K_r represents the stiffness of the aluminum pushrod, M is the deadweight on the sample, and C represents the overall damping present in the system. The base motion is represented by x, and the top motion is represented by y.

The overall stiffness of the system is given by

$$K = \frac{K_s K_r}{K_s + K_r}. \tag{1}$$

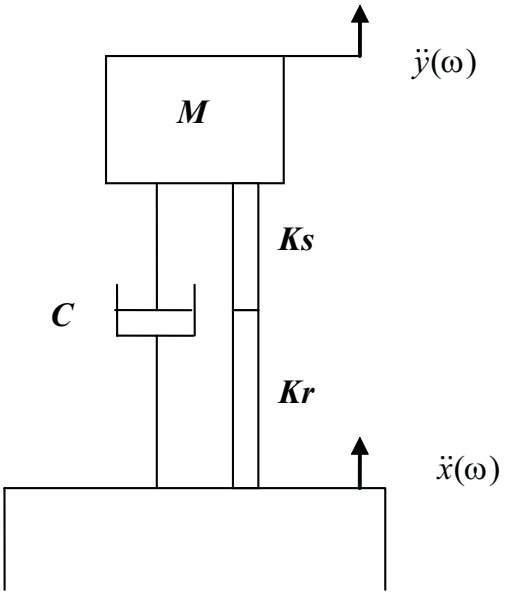

Figure 4. Schematic second order system used for characterization of the Ni-Mn-Ga material.

Downloaded From: http://proceedings.spiedigitallibrary.org/ on 07/12/2017 Terms of Use: http://spiedigitallibrary.org/ss/termsofuse.aspx

The natural frequency has the form

$$\omega_n = \frac{1}{2\pi}\sqrt{\frac{K}{M}}. \tag{2}$$

If the base is excited with frequency ω, the magnitude of the transmissibility relating the top acceleration to the base acceleration has the form

$$\left|\frac{\ddot{y}}{\ddot{x}}\right| = G = \frac{\sqrt{1+(2\zeta\frac{\omega}{\omega_n})^2}}{\sqrt{[1-(\frac{\omega}{\omega_n})^2]^2+(2\zeta\frac{\omega}{\omega_n})^2}}, \tag{3}$$

where ζ is the overall damping ratio of the system. Defining the maximum transmissibility ratio G_{max} as the value of (3) at resonance frequency ω_n, the damping and stiffness can be calculated through the following expressions

$$\zeta = \frac{1}{2}\sqrt{\frac{1}{G_{max}^2-1}}, \tag{4}$$

$$K_s = \frac{M(2\pi\omega_n)^2 K_r}{Kr - M(2\pi\omega_n)^2}. \tag{5}$$

4. RESULTS AND DISCUSSION

4.1. Collinear Field Tests

The transmissibility ratio transfer function relating the acceleration of the top to the acceleration of the base provides information on the resonance frequency and damping present in the system. The measurements obtained in the collinear field configuration are shown in Figure 5. The sample exhibits only two distinct resonances after subjecting it to several fields ranging from 0 to 430 kA/m: at fields below 330 kA/m, the sample exhibits a resonance frequency of approximately 1913 Hz; at fields of more than 330 kA/m, the resonance is observed at 2299 Hz. These results point to an ON/OFF effect with a threshold field of 330 kA/m. This result was validated through repeated runs under the same conditions, as shown in Figure 6, which shows the two distinct resonances for three different tests as well as model calculations. The stiffness of the aluminum pushrod used in these tests is 1.36e8 N/m, and the mass of the dead weight is 60.97 g. The two average stiffnesses calculated with expression (5) are K_{s1} = 9.10e6 N/m and K_{s2} = 1.38e7 N/m. The average damping ratios calculated with expression (4) are $\zeta_1 = 0.0286$ and $\zeta_2 = 0.0408$. The average field at which the shift takes place is 285 kA/m. One of the possible reasons for the slight variation in the field at which the threshold occurs is the position of the sample with respect to the solenoid. If the sample is not exactly aligned along the length of the solenoid, the field might be slightly tilted. This can give rise to varied magnitudes of field even when the current in the solenoid is the same. Since the sample exhibits only ON/OFF behavior, this problem can be easily overcome through the application of a slightly higher amount of field than that observed in the experiments. A field of 330 kA/m can be considered optimum for achieving the second resonance frequency as compared to the resonance at lower fields. The results of the collinear tests are summarized in Table 1. It is seen that there is an average resonance shift of 21.3% and an average stiffness shift of around 51.5%, both relative to the zero-field value.

Table 1. Summary of collinear field test results.

Run #	ω_{n1}(Hz)	ω_{n2}(Hz)	% change	K_{s1}(N/m)	K_{s2}(N/m)	% change	ζ_1	ζ_2	% change
1	1913	2299	**20.2**	9.25e6	1.37e7	**48.1**	0.033	0.047	**42.4**
2	1948	2390	**22.7**	9.62e6	1.50e7	**55.9**	0.024	0.035	**45.8**
3	1831	2217	**21.1**	8.43e6	1.27e7	**50.6**	0.029	0.040	**37.9**
Average			**21.3**			**51.5**			**42.0**

Downloaded From: http://proceedings.spiedigitallibrary.org/ on 07/12/2017 Terms of Use: http://spiedigitallibrary.org/ss/termsofuse.aspx

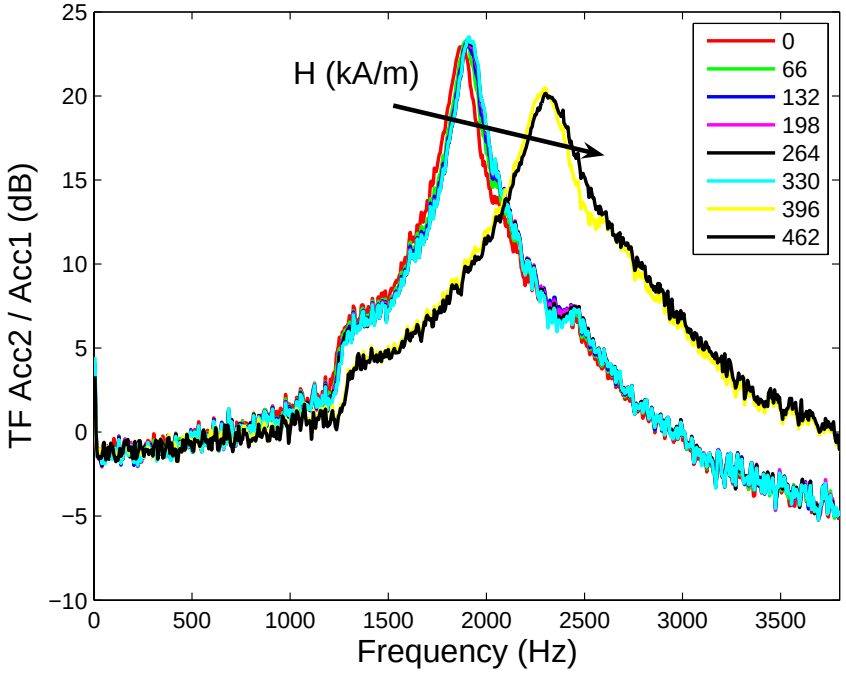

Figure 5. Acceleration transmissibility with collinear field.

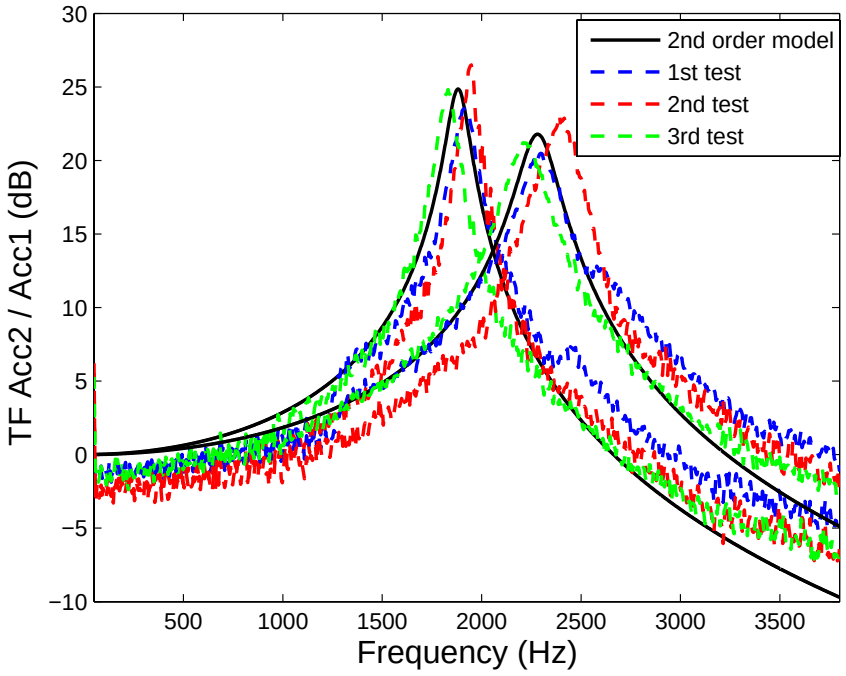

Figure 6. Collinear field test model results and repeated measurements under the same field inputs.

Downloaded From: http://proceedings.spiedigitallibrary.org/ on 07/12/2017 Terms of Use: http://spiedigitallibrary.org/ss/termsofuse.aspx

The stiffness increases with increasing field since the sample is initially in its field-preferred, mechanically softest state. Although the damping ratios also show a large average shift of about 42.0%, the damping values are small at all magnetic fields. This is beneficial for the implementation of Ni-Mn-Ga in tunable vibration absorbers with a targeted absorption frequency.

4.2. Transverse field Tests

The measurements conducted in the transverse field case are shown in Figure 7. Two differences with respect to the collinear tests are observed. First, since the sample is initially configured in its stiffest state as a single stress-preferred variant, an increase in transverse magnetic field produces a decrease in the mechanical stiffness and associated resonance frequency. Secondly, the material exhibits a gradual change in resonance frequency with changing field, in this case from values of around 2290 Hz for zero applied field to around 1460 Hz for a dc magnetic field of 423 kA/m. The three panels in Figure 7 show three different runs conducted on the sample. It is seen that the overall frequency magnitudes are about 5% different for test (b). The frequency shifts for the three cases are -36.4%, -33.0%, and -35.9%, giving an average shift of -35.1%.

The overall resonance frequency shift and sample stiffness shift in the transverse field tests are higher than in the collinear field test. For the collinear measurements, the average stiffness in the stress-preferred configuration is 1.38e7 N/m, whereas for the transverse tests it is 1.34e7 N/m. However, the average stiffness when the sample

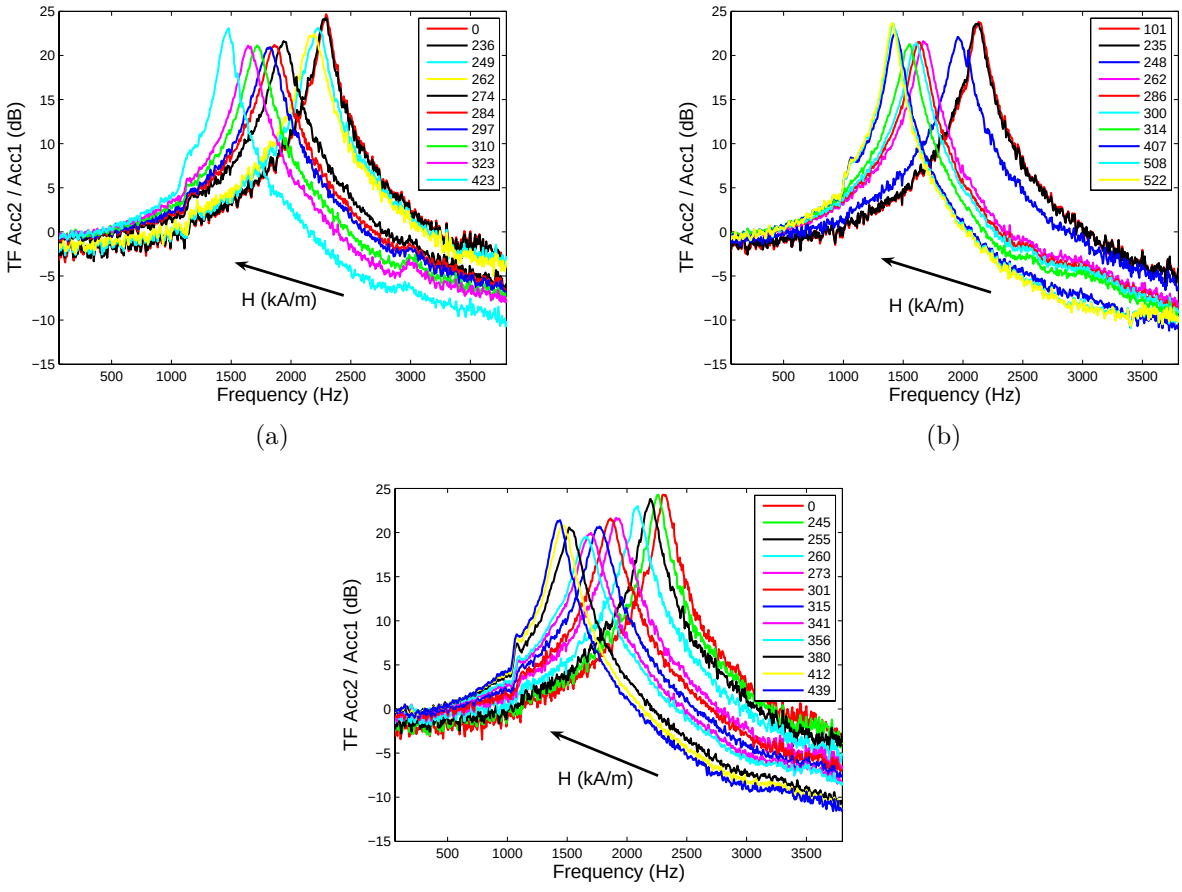

Figure 7. Transmissibility ratio measurements. (a), (b), and (c) denote three different runs conducted on the same sample.

Downloaded From: http://proceedings.spiedigitallibrary.org/ on 07/12/2017 Terms of Use: http://spiedigitallibrary.org/ss/termsofuse.aspx

is supposed to be in the completely field-preferred state is 9.1e6 N/m in the case of collinear field tests and 5.27e6 N/m in the case of transverse field tests. This state occurs at the start for the collinear field test and at the end in the transverse field test. The possible reason behind this difference is that the manual pressure applied while mounting the sample for collinear field tests results in initiation of twin boundary motion and a certain fraction of the sample is transformed into the stress-preferred variant. This results in an increased stiffness as compared to a completely field-preferred configuration. However, this behavior is consistent in the three runs indicating that the structure assumed by the sample had been nearly the same during the tests.

The sample stiffness and overall system damping ratio are calculated by using equations (1) to (5). Table 2 shows the resonance frequency, stiffness, and damping ratio variation in extreme values for the transverse field tests. The aluminum pushrods used in these tests have different dimensions than those used in the collinear measurements, and hence the stiffness has a different value of 1.068e7 N/m. The dead weight has the same mass of 60.87 g. The dependence on initial bias field of the measured resonance frequency, calculated stiffness, and calculated damping ratio of the system are illustrated in Figures 8-11. The average stiffness shift considering all three runs is -60.7%.

The damping ratios show small overall magnitudes, hence implying that the sample is suitable for tunable vibration absorption applications. Figures 9 and 11 show that the transmissibility ratio and damping ratio are relatively flat over the bias fields considered when compared with the resonance frequency and stiffness. The slight rise and drop in the damping can be attributed to the presence of twin boundaries.[10] With increasing field, the field-preferred twin variants are initiated with the introduction of the twin boundaries between the two variants. With increasing fields, the twin boundaries continue to exist, resulting in constant or increased damping. At higher bias fields, when the sample is completely in its field-preferred variant configuration, the number of twin boundaries decreases resulting again in lower damping. This trend is clearly seen in runs (a) and (b), but less so in run (c).

Because of the relatively high demagnetization factor (0.385) in the transverse direction, it takes higher external fields to fully elongate the sample. Thus, a continuous change of resonance frequency and hence stiffness is observed with increasing bias fields. In the case of the collinear field tests, the demagnetization factor is 0.229. Thus, once the twin boundary motion starts, it takes a very small range of fields to transform the sample fully into the stress-preferred state. Thus, an abrupt change in the resonance frequency and hence stiffness is seen in the collinear field tests.

5. CONCLUDING REMARKS

The single-crystal Ni-Mn-Ga sample characterized in this paper exhibits varied dynamic stiffness with changing bias fields. The non-contact method of applying the magnetic fields ensures consistent testing conditions. This is an improvement over our prior work,[7] in which permanent magnets were used to apply magnetic fields along the longitudinal direction. Unlike that study, the characterization presented here was conducted on commercial Ni-Mn-Ga material, under both collinear and transverse configurations. The field is not applied throughout the duration of a given test, but only initially in order to transform the sample into a given twin variant configuration. The overall resonance frequency and stiffness change in the transverse field tests are -35.1% and -60.7% respectively. The equivalent values for the collinear field tests are 21.3% and 51.5%, respectively. The

Table 2. Summary of transverse field test results.

Run #	ω_{n1}(Hz)	ω_{n2}(Hz)	% change	K_{s1}(N/m)	K_{s2}(N/m)	% change	ζ_1	ζ_2	% change
1	2294	1460	**-36.4**	1.41e7	0.53e7	**-62.5**	0.030	0.037	**24.5**
2	2147	1439	**-33.0**	1.21e7	0.51e7	**-57.7**	0.032	0.037	**15.5**
3	2294	1470	**-35.9**	1.41e7	0.54e7	**-61.9**	0.030	0.046	**55.6**
Average			**-35.1**			**-60.7**			**31.8**

Downloaded From: http://proceedings.spiedigitallibrary.org/ on 07/12/2017 Terms of Use: http://spiedigitallibrary.org/ss/termsofuse.aspx

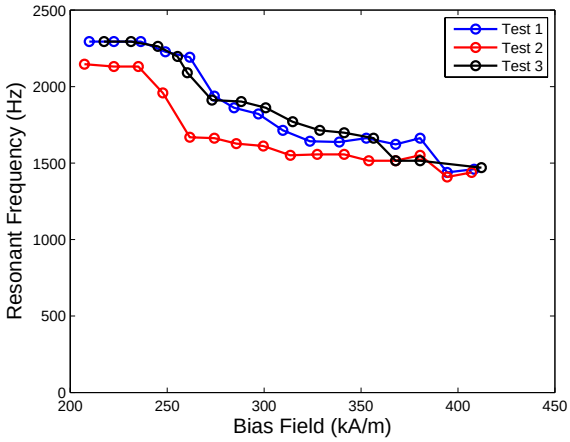

Figure 8. Resonance frequency vs. initial bias field.

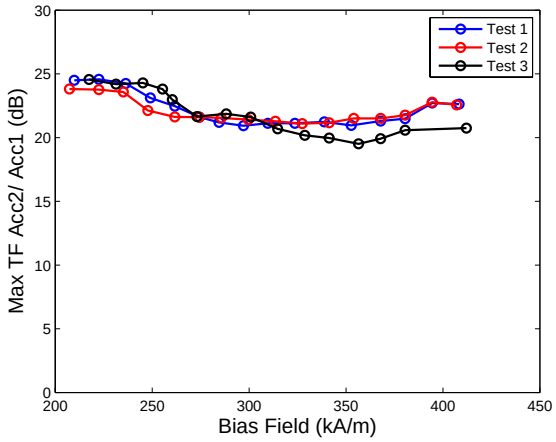

Figure 9. Maximum transmissibility vs. initial bias field.

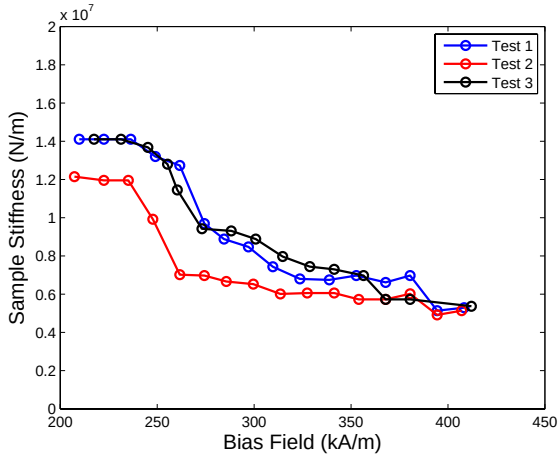

Figure 10. Sample stiffness vs. initial bias field.

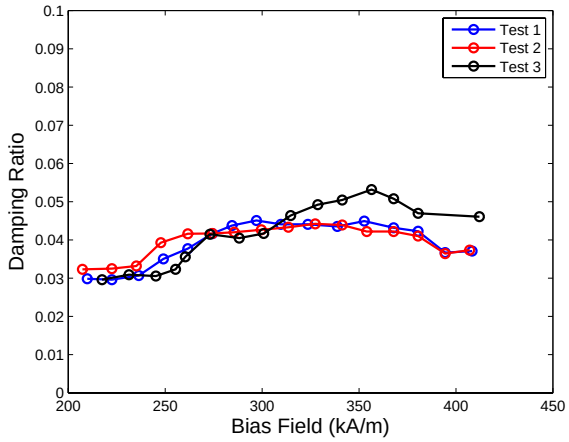

Figure 11. Minimum damping ratio vs. initial bias field.

damping values observed in the tests are small (≈ 0.03)and are conducive to the use of Ni-Mn-Ga in active vibration absorbers.

The sample shows an ON/OFF behavior in the collinear field tests, whereas a continuously changing resonance frequency is observed in the transverse field tests. Thus, depending on the application and the frequency range under consideration, the sample can be operated either in transverse or collinear field configuration. The transverse field configuration offers more options regarding the ability to select a particular resonance frequency. The collinear field configuration only offers two discrete resonance frequencies but can be devised in a more compact manner.

The sample behavior can be modeled by assuming a discretized second order system. However, the development of a continuous dynamic model is desirable for handling different sample geometries and higher modes. Although in this study the magnetic field was switched off during the dynamic tests, development of a model with the sample immersed in an external magnetic field during testing might be useful for creating a more complete characterization of the dynamic behavior exhibited by Ni-Mn-Ga.

Downloaded From: http://proceedings.spiedigitallibrary.org/ on 07/12/2017 Terms of Use: http://spiedigitallibrary.org/ss/termsofuse.aspx

Acknowledgement

The authors wish to acknowledge the financial support of the National Science Foundation through grant CMS-0409512, Dr. Shih-Chi Liu program director.

REFERENCES

1. P. Mullner, V. Chernenko, and G. Kostorz, "Stress-induced twin rearrangement resulting in change of magnetization in a NiMnGa ferromagnetic martensite," *Scripta Materialia*, **49**, pp. 129-133 (2003).
2. L. Straka, and O. Heczko "Superelastic Response of NiMnGa Martensite in Magnetic Fields and a Simple Model," *IEEE Transactions on Magnetics*, **39**, 5, pp. 3402-3404 (2003).
3. O. Heczko, "Magnetic shape memory effect and magnetization reversal," *Journal of Magnetism nad Magnetic Materials*, **290-291**, pp. 787-794 (2005).
4. G. Li, Y. Liu, and B. K. A. Nogi, "Some aspects of strain-induced change of magnetization in a NiMnGa single crystal," *Scripta Materialia*, **53** pp. 829-834 (2005).
5. I. Suorsa, E. Pagounis, and K. Ullakko, "Magnetization dependence on strain in the NiMnGa magnetic shape memory material," *Applied Physics Letters*, **84**, 23, pp. 4658-4660 (2004).
6. N. Sarawate, and M. Dapino, "Experimental characterization of the sensor effect in ferromagnetic shape memory Ni-Mn-Ga," *Applied Physics Letters*, **88**, pp. 121923 (2006).
7. L. Faidely, M. Dapino, G. Washington, and T. Lograsso, "Modulus increase with magnetic field in ferromagnetic shape memory NiMnGa," *Journal of Intelligent Material Systems and Structures*, **17**, 2, pp. 123-131 (2006).
8. A. Malla, M. Dapino, T. Lograsso, and D. Schlagel, "Effect of composition on the magnetic and elastic properties of shape memory Ni-Mn-Ga," *Proceedings of SPIE*, **5053-29**, (2003).
9. C. Henry, "Dynamic actuation properties of Ni-Mn-Ga ferromagnetic shape memory alloys", PhD Thesis, MIT, (2002).
10. E. Gans, C. Henry, and G. Carman, "High Energy Absorption in bulk ferromagnetic shape memory alloys ($Ni_{50}Mn_{29}Ga_{21}$)," *Proceedings of SPIE*, **5387**, pp. 177-185 (2004).

Downloaded From: http://proceedings.spiedigitallibrary.org/ on 07/12/2017 Terms of Use: http://spiedigitallibrary.org/ss/termsofuse.aspx